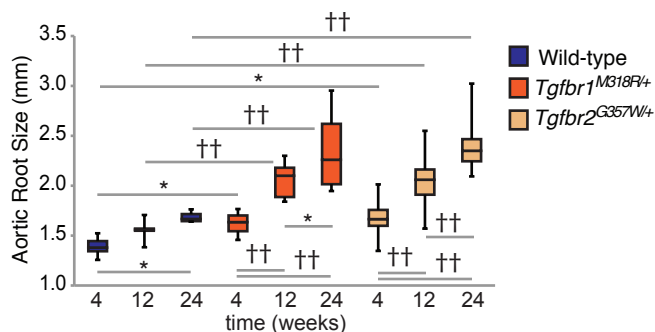


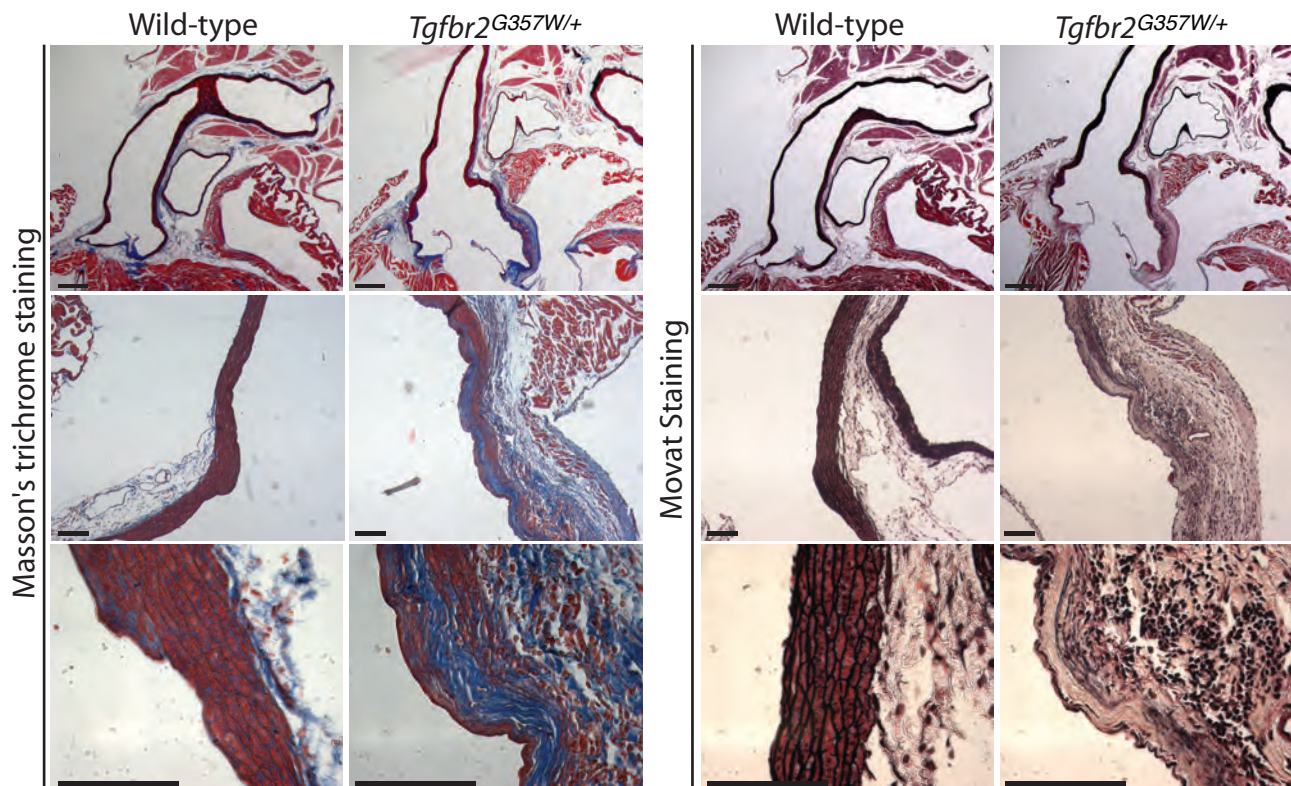
A

Genotype	4 weeks	24 weeks
Wild-type	1.4 (0.1)	1.7 (0.1)
<i>Tgfb1</i> <sup>+/-</sup>	1.5 (0.1)	1.7 (0.1)
<i>Tgfb2</i> <sup>+/-</sup>	1.5 (0.1)	1.8 (0.1)
<i>Tgfb1</i> <sup>M318R/+</sup>	1.7 (0.2)	2.3 (0.4)
<i>Tgfb2</i> <sup>G357W/+</sup>	1.7 (0.2)	2.3 (0.3)

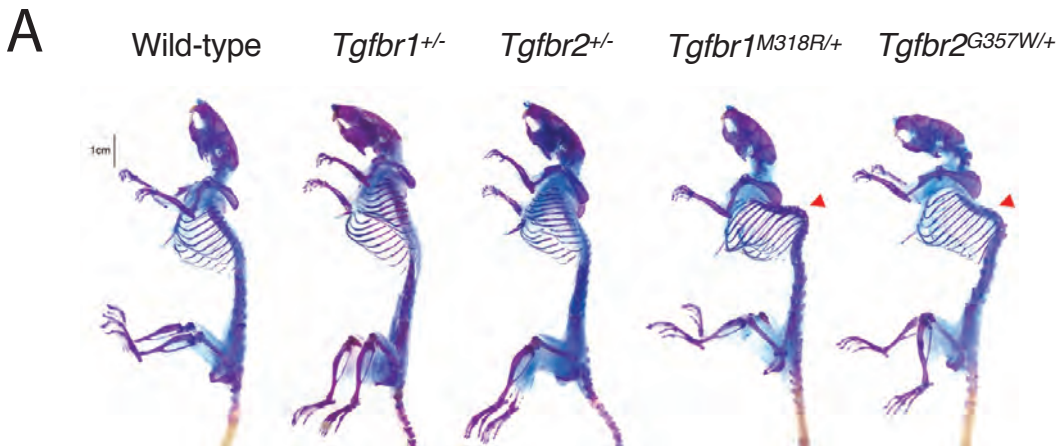
B



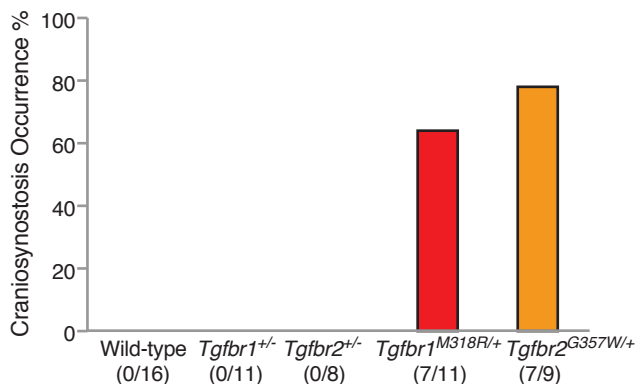
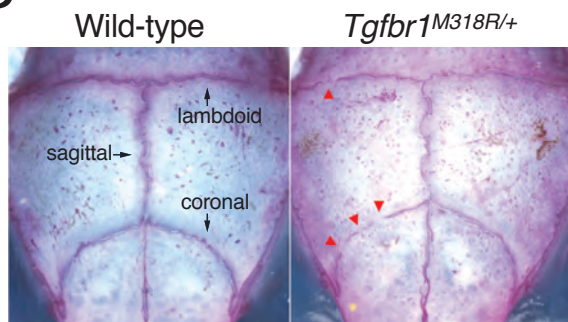
C



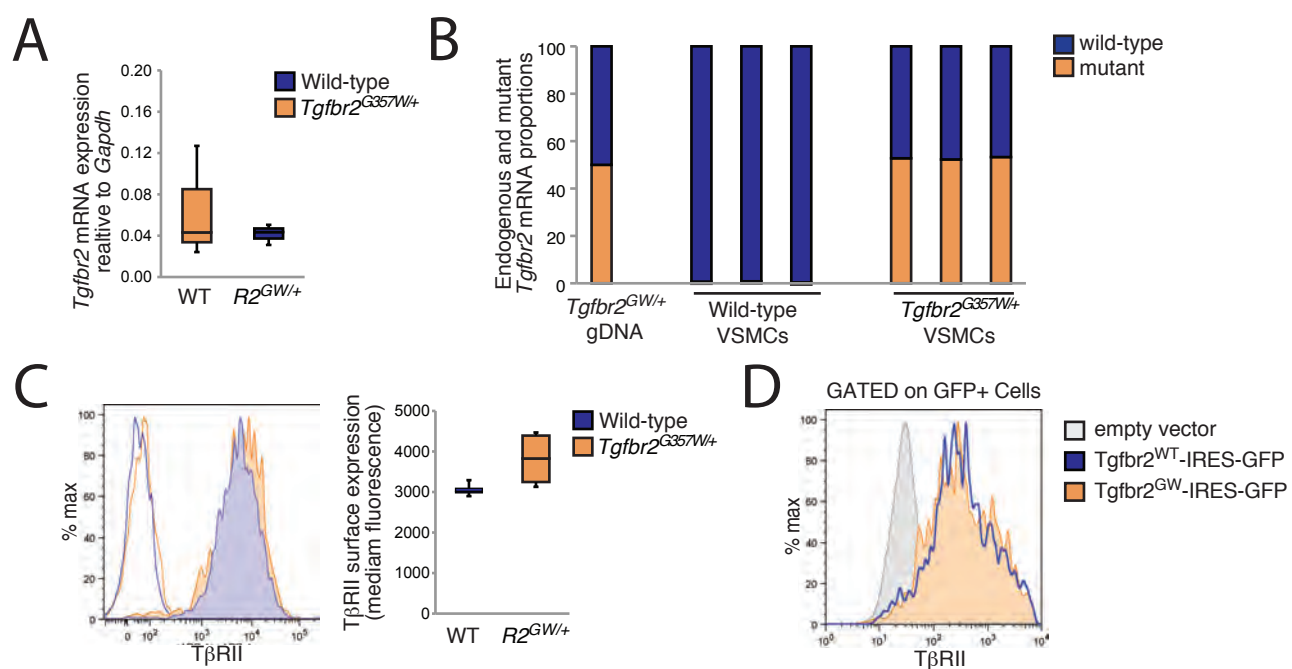
**Supplementary Figure 1. Progressive worsening of aortic root aneurysm in knock-in LDS mutant mice but not in TGFβ receptor haploinsufficient mice** (A) Average aortic root size at 4 and 24 weeks as measured by echocardiography in control, TGFβ receptor haploinsufficient mice and knock-in LDS mouse models; standard deviation is shown in parenthesis, (n≥9). (B) Aortic root size at 4, 12 and 24 weeks of age as measured by echocardiography in wild-type and knock-in LDS mutant mice, (n ≥9). \*P< 0.05, \*\*P< 0.00005 (C) Representative images of 36 week old control and *Tgfb2*<sup>G357W/+</sup> mice aortas stained with Masson's trichrome (right) and Movat staining (left). Scale bars are 500 μm (top panel) and 100 μm (middle and bottom panel).



**B**

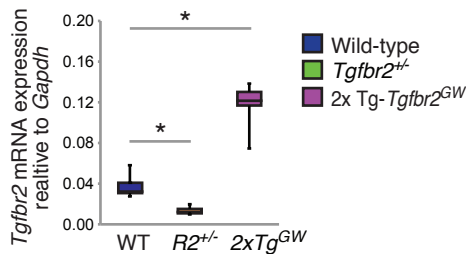


**Supplementary Figure 2. Skeletal phenotype of LDS knock-in and haploinsufficient mouse models.** (A) Representative alcian blue and alizarin red staining of 24 week old mouse skeletons. Kyphosis (over-curvature of the spine) as indicated by the red arrows is evident in both knock-in LDS mouse strains, whereas haploinsufficient mice show no obvious skeletal abnormalities at this age when compared to wild-type littermates. (B) Alcian blue and alizarin red staining of 8 week old wild-type and *Tgfr1*<sup>M318R/+</sup> mouse skulls to highlight the sagittal, lambdoid and coronal cranial sutures. Patchy closure of the coronal and lambdoid sutures is evident in the *Tgfr1*<sup>M318R/+</sup> knock-in mouse as indicated by the red arrows. Graphs shows incidence of craniosynostosis in haploinsufficient and LDS knock-in mice.

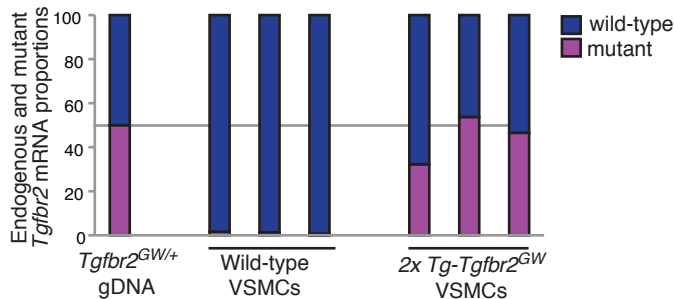


**Supplementary Figure 3. Characterization of *Tgfr2* mRNA and TβRII protein expression in VSMCs cultures derived from control and *Tgfr2*<sup>G357W/+</sup> LDS knock-in mice.** (A) Expression of *Tgfr2* mRNA in control and *Tgfr2*<sup>G357W/+</sup> VSMCs as evaluated by qPCR and normalized to that of *Gapdh*, (n= 3). (B) Expression of the mutant *Tgfr2*<sup>G357W</sup> transcript was assessed by pyrosequencing in control and *Tgfr2*<sup>G357W/+</sup> VSMCs. Pyrosequencing was also performed on genomic DNA from a *Tgfr2*<sup>G357W/+</sup> mouse to correct for allele-specific pyrosequencing efficiency (C) Surface expression of TβRII in control and *Tgfr2*<sup>G357W/+</sup> VSMCs as evaluated by flow cytometry using an antibody directed against TβRII (filled histograms) or isotype control antibody (open histograms), (n= 3). (D) Surface expression of TβRII in RII-null T47D cells transfected with constructs encoding for wild-type and *Tgfr2*<sup>G357W</sup> cDNA followed by IRES-GFP.

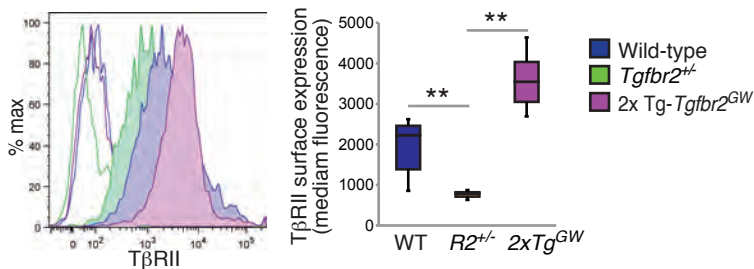
A



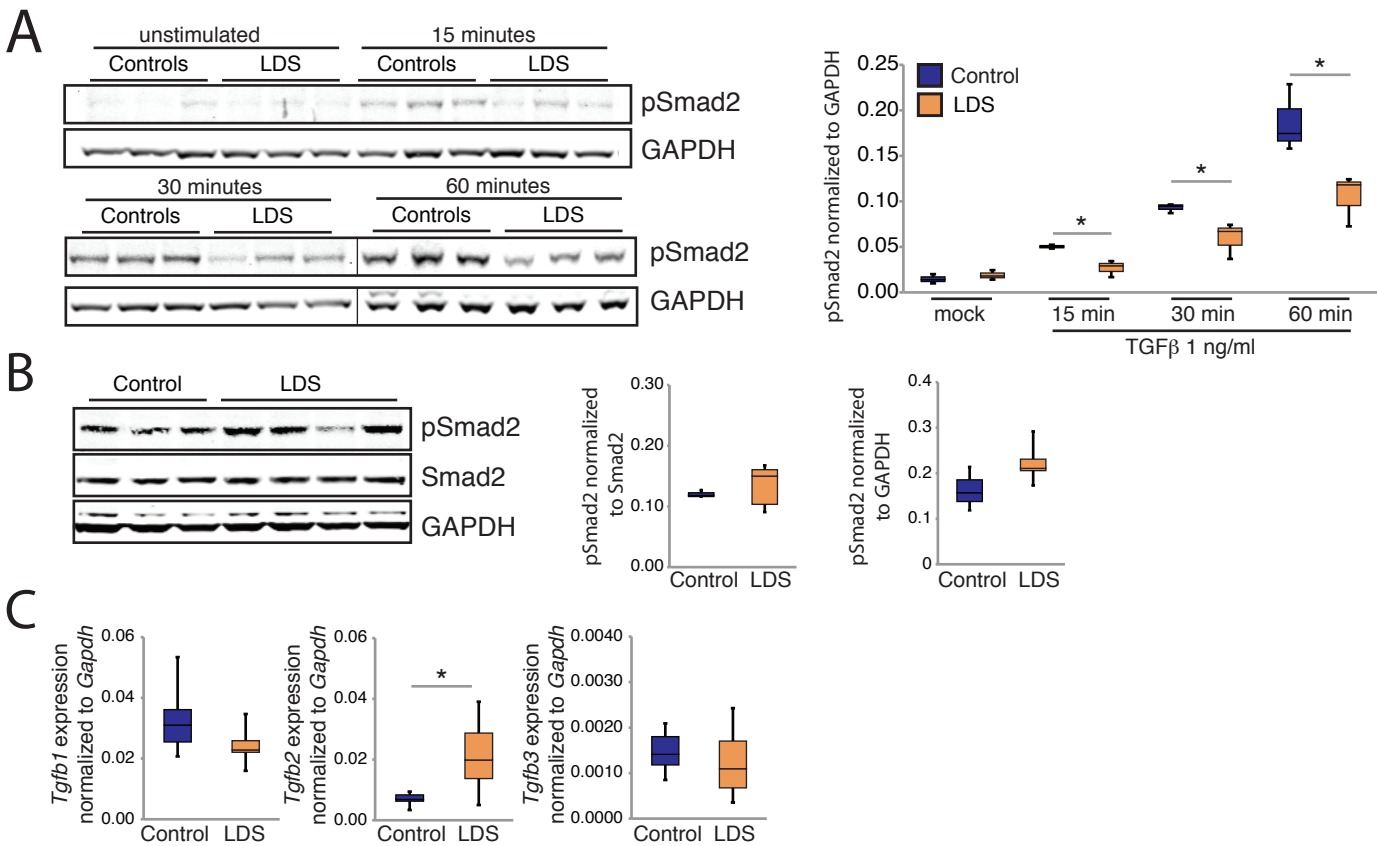
B



C

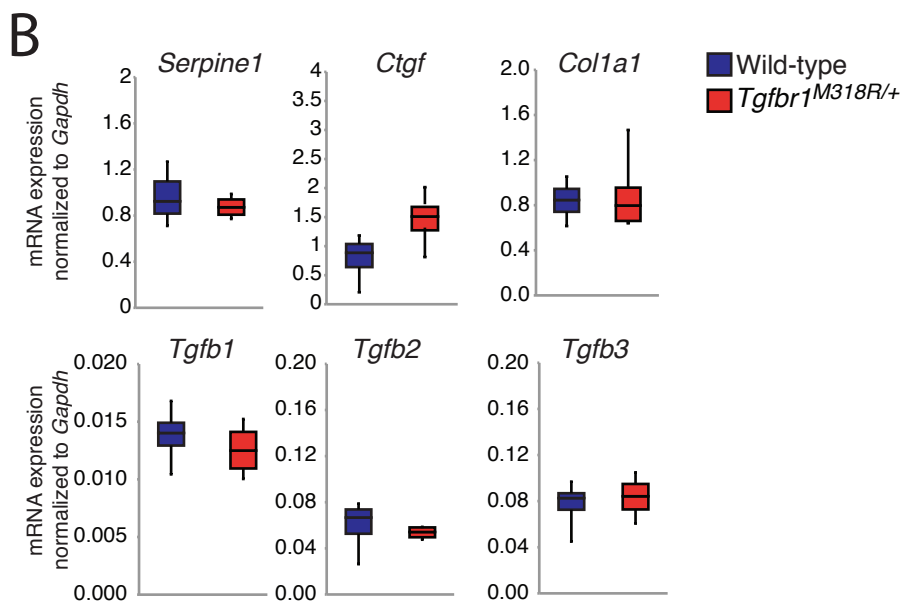
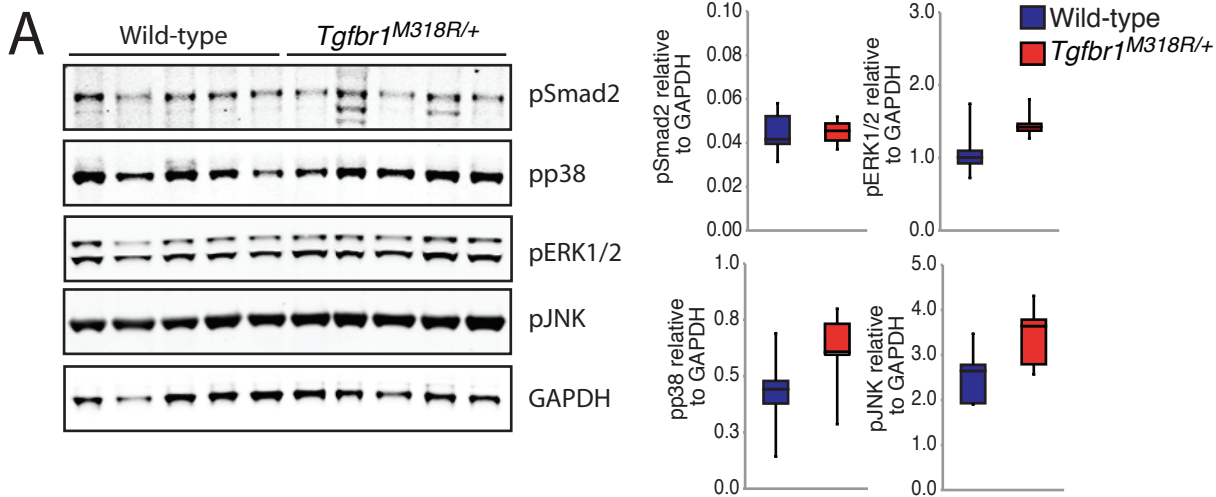


**Supplementary Figure 4. Characterization of *Tgfr2* mRNA and TβRII protein expression in VSMCs cultures derived from control, *Tgfr2*<sup>+/-</sup> haploinsufficient mice and 2x *Tgfr2*<sup>GW</sup> Transgenic mice.** (A) Expression of *Tgfr2* mRNA in control, *Tgfr2*<sup>+/-</sup> and 2x *Tgfr2*<sup>GW</sup> VSMCs as evaluated by qPCR and normalized to that of *Gapdh*, (n = 3). (B) Expression of the mutant *Tgfr2*<sup>G357W</sup> transcript was assessed by pyrosequencing in control and 2x *Tgfr2*<sup>GW</sup> VSMCs. Pyrosequencing was also performed on genomic DNA from a *Tgfr2*<sup>G357W/+</sup> mouse to correct for allele-specific pyrosequencing efficiency. (C) Surface expression of TβRII in control, *Tgfr2*<sup>+/-</sup> and 2x *Tgfr2*<sup>GW</sup> VSMCs as evaluated by flow cytometry using an antibody directed against TβRII (filled histograms) or isotype control antibody (open histograms), (n = 3). \**P* < 0.05, \*\**P* < 0.005.

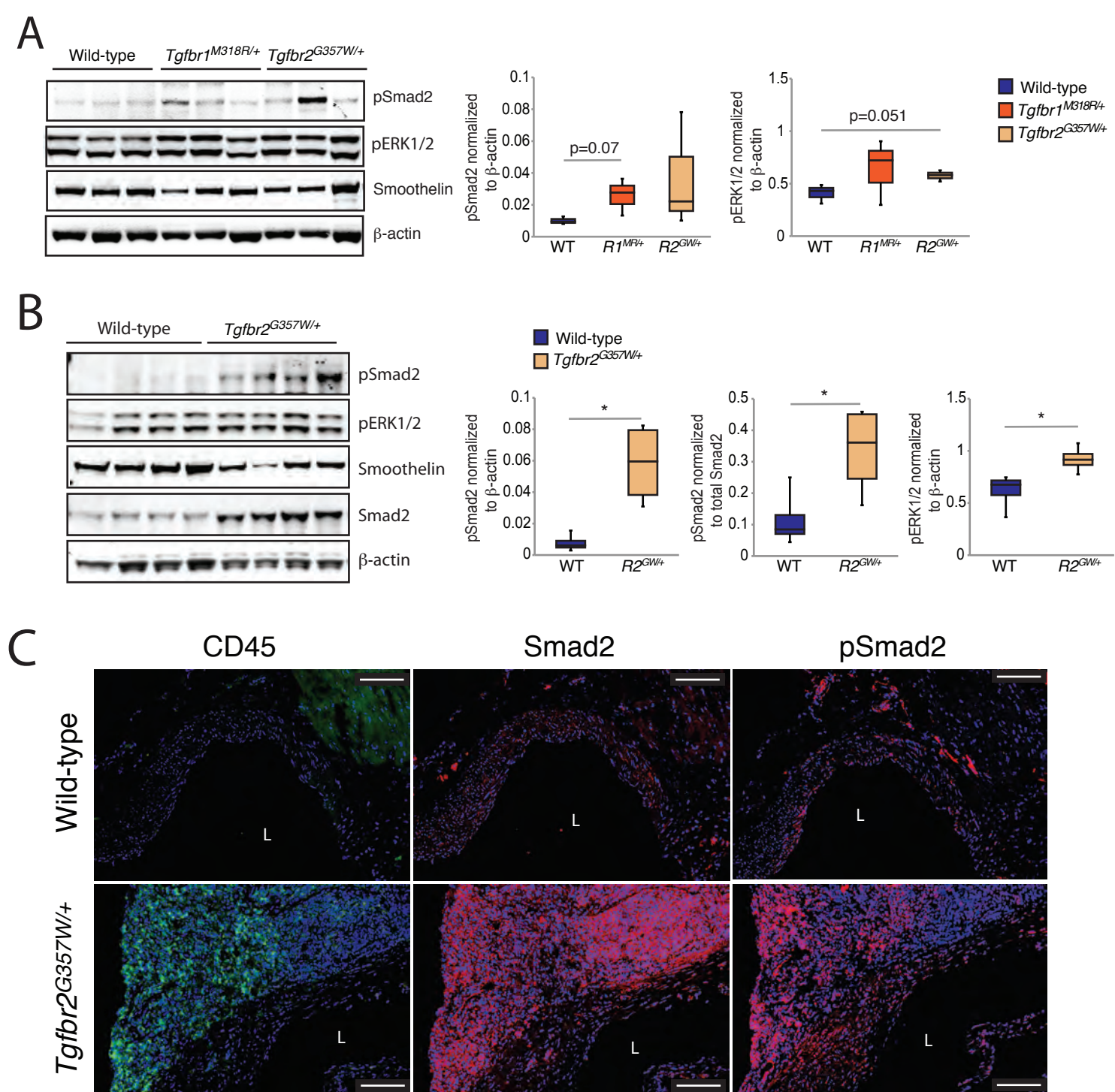


**Supplementary Figure 5. Defective phosphorylation of Smad2 in response to exogenous TGF $\beta$  but not under normal culture conditions in VSMCs derived from LDS patients.**

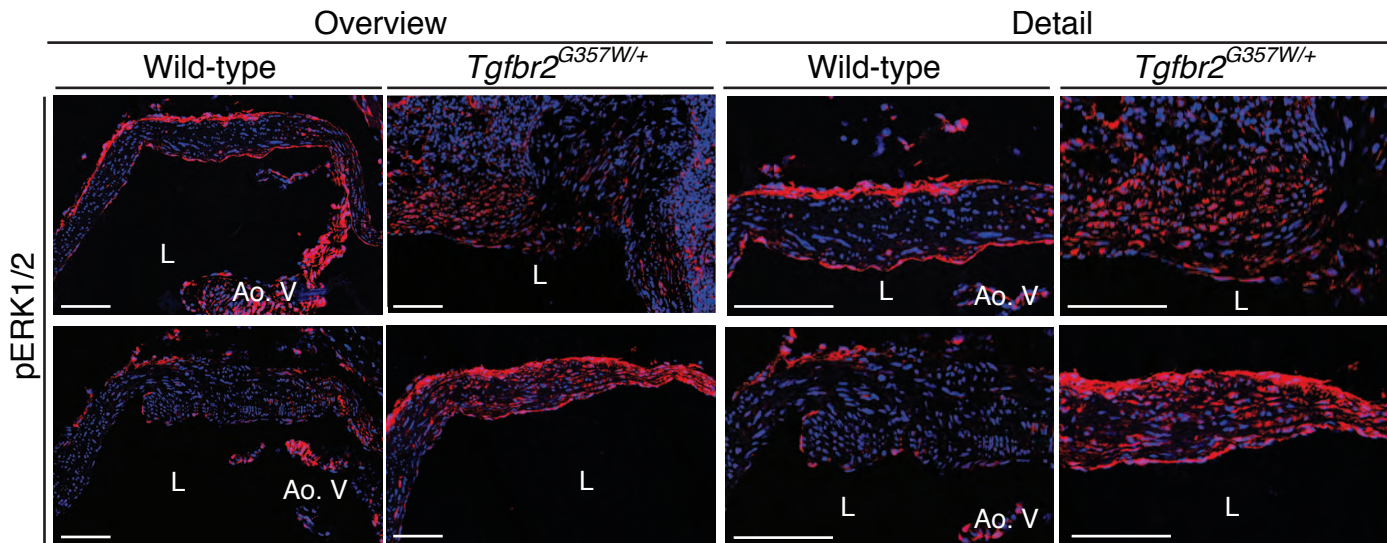
(A) Defective induction of Smad2 phosphorylation in response to exogenous TGF $\beta$  in VSMCs derived from LDS patients. VSMCs were starved overnight in 2% serum and stimulated for the indicated time-points with 1 ng/ml TGF $\beta$ 1. LDS VSMCs used for this experiment were derived from patients carrying the following mutations: R528H in *TGFBR2*; A329T in *TGFBR2*; L354P in *TGFBR1*, (n=3). (B) Levels of Smad2 phosphorylation in unstimulated VSMCs derived from LDS patients and controls. VSMCs were grown in 5% serum to approximately 80% confluence prior to analysis. LDS VSMCs used for this experiment were derived from patients carrying the following mutations: L354P in *TGFBR1*; R528H in *TGFBR2*; A329T in *TGFBR2*; G353V in *TGFBR1* (n=3 for controls, n=4 for LDS). (C) Analysis of *Tgfb1*, *Tgfb2* and *Tgfb3* expression in VSMCs derived from control and LDS patients cultured as in B. VSMCs used for this experiment were derived from patients carrying the following mutations: R528H (2 patients), R528C (2 patients), and G351D in *TGFBR2*; L354P and G353V in *TGFBR1* gene (n=7).



**Supplementary Figure 6. Normal TGF $\beta$  signaling in knock-in LDS mouse models at 8 weeks of age.** (A) Western blot analysis of protein lysates derived from the aortic root of 8 weeks old *Tgfb1<sup>M318R/+</sup>* and control mice showing normal levels of canonical and non-canonical TGF $\beta$  signalling intermediates. (B) Normal expression of TGF $\beta$  ligands and TGF $\beta$  gene targets in aortic root samples from 8 weeks old *Tgfb1<sup>M318R/+</sup>* mice as evaluated by qPCR and normalized to that of *Gapdh*, (n= 4).

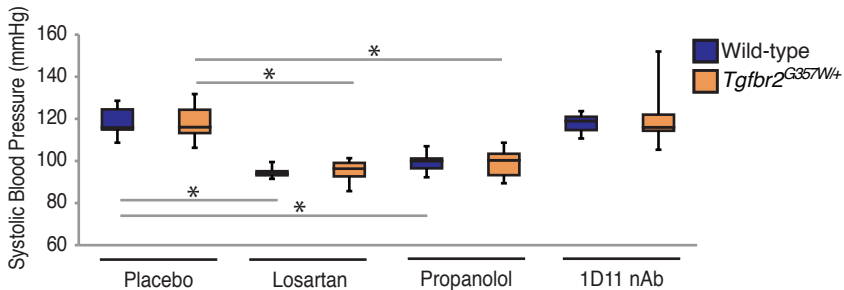


**Supplementary Figure 7. Smad2 and ERK phosphorylation in knock-in LDS mouse models at 24 and 36 weeks of age.** (A) Western blot analysis of protein extracts derived from the aortic root of 24 week old *Tgfr1<sup>M318R/+</sup>*, *Tgfr2<sup>G357W/+</sup>* and control mice showing normal or increased levels of pSmad2 and pERK in LDS samples. (B) Western blot analysis of protein extracts derived from the aortic root of 36 week old *Tgfr2<sup>G357W/+</sup>* and control mice showing increased levels of pSmad2 and pERK in *Tgfr2<sup>G357W/+</sup>* samples. (C) Representative long axis view images showing elevated levels of pSmad2 and total Smad2 in the adventitial layer of *Tgfr2<sup>G357W/+</sup>* at 24 weeks of age. Images were acquired as a tile with a 25X magnification. L=lumen. Scale bars are 100  $\mu$ m.\* $P \leq 0.05$ .



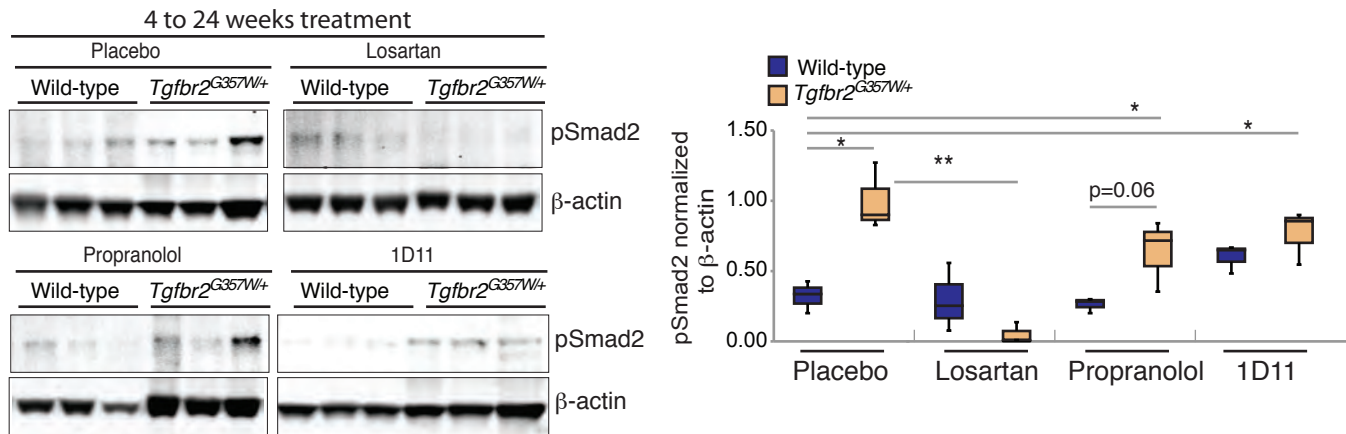
**Supplementary Figure 8. Increased ERK phosphorylation in the medial layer of the aortic root of LDS mice at 24 weeks of age.** Representative long axis view images of pERK1/2 staining in the aortic root of 24 week old *Tgfb<sup>r2</sup><sup>G357W/+</sup>* and control mice as assessed by immunofluorescence. L, lumen; Ao. V, aortic valve. Images were acquired as a tile with a 25X magnification. Scale bars are 100  $\mu$ m.



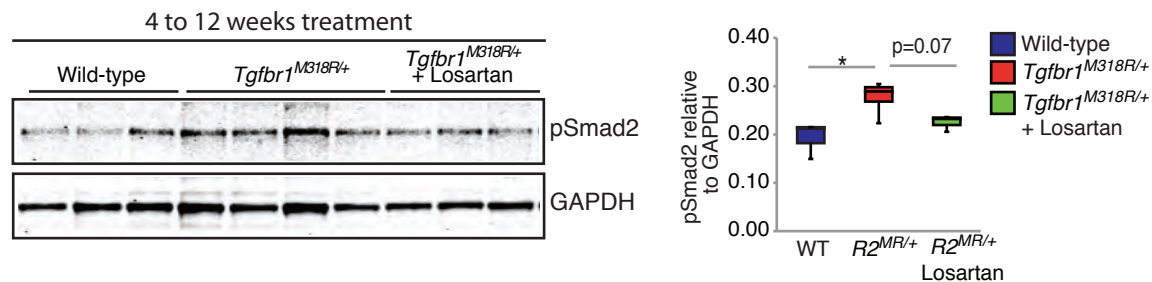


**Supplementary Figure 9. Blood pressure of *Tgfbr2*<sup>G357W/+</sup> and control mice treated with placebo, losartan, propranolol or 1D11 nAb.** Losartan and propranolol reduced blood pressure to equivalent levels, (n≥8). \*P ≤ 0.05.

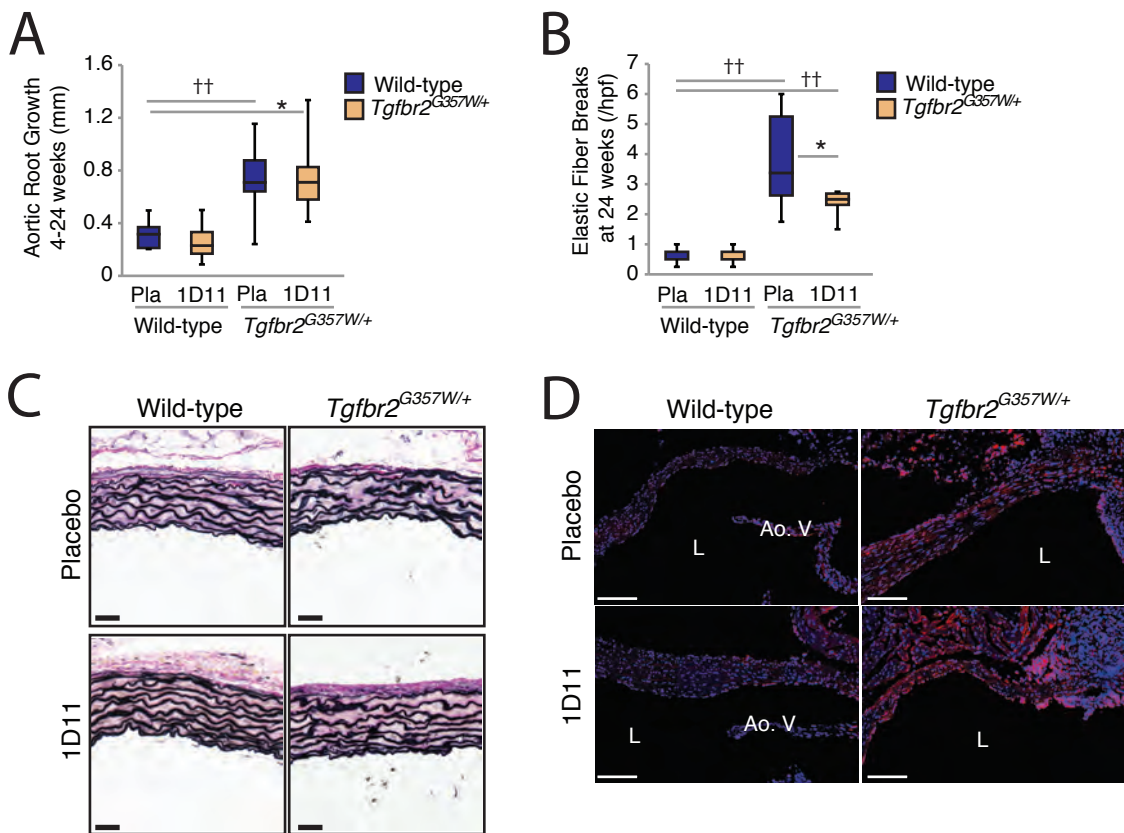
A



B



**Supplementary Figure 10. Reduction of Smad2 phosphorylation correlates with therapeutic efficacy of losartan.** (A) Western blot analysis of aortic root lysates derived from 24 week old LDS and control mice treated with placebo, losartan, propranolol or the 1D11 NAB starting at 4 weeks of age. Treatment with losartan reduced Smad2 phosphorylation, while propranolol and 1D11 nAb failed to do so. (B) Western blot analysis of aortic root lysates derived from 12 week old LDS and control mice treated with placebo or losartan starting at 4 weeks of age. \* $P \leq 0.05$ , \*\* $P \leq 0.005$ .



**Supplementary Figure 11. Partial amelioration of elastic fiber breaks by treatment with 1D11 antibody.** (A) Aortic root growth from 4 to 24 weeks of age as measured by echocardiography in  $Tgfr2^{G357W/+}$  and control mice treated with the 1D11 antibody or left untreated, ( $n \geq 8$ ) (B) Quantification of elastic fiber breaks per hpf in 24 week old untreated and 1D11-treated  $Tgfr2^{G357W/+}$  and control mice, ( $n \geq 8$ ). (C) VVG staining of representative sections of the proximal ascending aorta of 24 week old untreated and 1D11-treated  $Tgfr2^{G357W/+}$  and control mice. Scale bars are 40  $\mu\text{m}$ . (D) Representative images of pSmad2 staining in the aortic root of 24 week old  $Tgfr2^{G357W/+}$  and control mice treated with 1D11 antibody. Images were acquired as a tile with a 25X magnification. L, lumen; Ao.V, aortic valve. Scale bars are 100  $\mu\text{m}$ . \* $P < 0.05$ , \*\* $P < 0.0005$ .